

Nickel Nanocone-Array Supported Silicon Anode for High-Performance Lithium-Ion Batteries

By Shichao Zhang,* Zhijia Du, Ruoxu Lin, Tao Jiang, Guanrao Liu, Xiaomeng Wu, and Dangsheng Weng

The development of Li-ion batteries with high capacity, long lifespan, and fast charge/discharge rates is of great technological importance for future portable electronics, power tools, electric and hybrid vehicles, and renewable energies.^[1–3] Silicon is a particularly appealing anode material for Li-ion batteries because of its high theoretical capacity of 4200 mAh g⁻¹^[4] and it has been the subject of extensive research efforts.^[5,6] However, lithium alloying and de-alloying with Si are accompanied by an enormous volume change (>300%), which induces severe pulverization and electrical disconnection from the current collector.^[7] This structural and electronic degradation thereby leads to drastic and fast capacity fading and hindrance of practical implementation. To overcome these drawbacks, one effective approach is to design powder-based composites (e.g., a Si-metal active/inactive matrix concept),^[8,9] preferably Si-carbon composites which have been investigated for many years.^[10–13] Previous research has shown improvement of the electrochemical performance of Si-based anodes but only to a limited extent.^[6] Alternatively, silicon anodes made of very thin films (a few tens of nanometers in thickness) have been reported to display a stable capacity over many cycles,^[14–16] whereas an increase in film thickness was urgently required to provide sufficient active material. Unfortunately, stress-induced cracking and the high inherent resistance of silicon lead to a poor cycling performance and rate capability owing to an increase in film thickness.^[6]

Recently, nanostructured silicon composites anodes with a specific layout were developed to address the above issues,^[17–20] in which an appropriate structure can provide the space to accommodate the volumetric change of the active silicon whereas an additional component facilitates the electron collection and transport. For instance, Yi Cui's group demonstrated anodes based on crystalline-amorphous core-shell Si nanowires (NWs) directly grown on metal current collectors.^[18] By limiting the charging potential above 150 mV versus lithium metal, the amorphous shells can be selectively used for lithium ion storage with excellent cycling stability and rate capability whereas the crystalline cores remain intact and function as efficient electron transport pathways and stable mechanical supports. However, these methods have some disadvantages such as comparatively

high synthesis costs, weak adhesion of the nanostructures to the substrate, and strict voltage control which is not feasible in practical Li-ion batteries.^[6]

Here we introduce a nickel nanocone-array (NCA) supported silicon anode architecture and demonstrate its meaningful improvement in cycling life and power rate for Li-ion batteries. **Figure 1** illustrates a typical preparation procedure of the electrode. The design includes uniform nickel NCAs as the electron collection and transport medium as well as the structural support and inactive confining buffer. A silicon coating is deposited on the NCAs as the electrochemical active material for lithium-ion storage. The NCAs supported Si anodes exhibit a relatively high reversible capacity of around 2640 mAh g⁻¹ with 88.7% capacity retention over 100 cycles. The excellent rate capability at 1 C and 2 C rates is also demonstrated in this report.

Figure 2A displays a representative scanning electron microscopy (SEM) image of the Ni NCAs showing their regularity. The bases of the cones show an average diameter of around 200 nm whereas the tips are very sharp with a distance of about 350 nm between them. The mean height of the cones is around 400 nm, and the surface of the cones is very rough. Larger and smaller cones are also observed in the mix. These robust Ni NCAs have previously been reported for their superhydrophobic and enhanced magnetic properties but, thus far, they have not been used for batteries.^[21,22] With the supporting substrate established, radiofrequency (rf) sputtering of Si on these cones is conducted afterwards to produce the electrode. Top and cross-sectional views (**Figure 2B** and its inset) reveal that the morphology of the resulting electrode is composed of many densely packed cylinders with regular dome-shapes at the top, indicating that the perpendicularly grown Ni cones are all covered by the Si coating.

The homogeneous Si/Ni structures were further confirmed by transmission electron microscopy (TEM, **Figure 2C**), which also showed that the thickness of the Si/Ni composites is approximately 650 nm (about 250 nm more than the height of Ni cones). The dispersed selected-area electron diffraction (SAED) pattern (**Figure 2D**) verifies that the rf-sputtered Si is completely amorphous. This is in accordance with the X-ray diffraction results which also show no Si crystal peaks (Supporting Information, **Figure S2**). A high-magnification TEM image of the Si/Ni structures (**Figure 2F**) distinctly manifests that the Ni cone is completely surrounded by the Si coating. High-resolution TEM indicated that the Ni cones are well crystallized with a distance of 0.203 nm between the neighboring lattice planes, which is in agreement with the *d*(111) spacing of face-centered cubic nickel (fcc-Ni). The interface of the amorphous Si layer

[*] Prof. S. Zhang, Z. Du, R. Lin, Dr. T. Jiang, G. Liu, X. Wu, Prof. D. Weng
School of Materials Science and Engineering
Beijing University of Aeronautics and Astronautics
Xueyuan Road, Haidian District, Beijing, 100191 (China)
E-mail: csc@buaa.edu.cn

DOI: 10.1002/adma.201003017

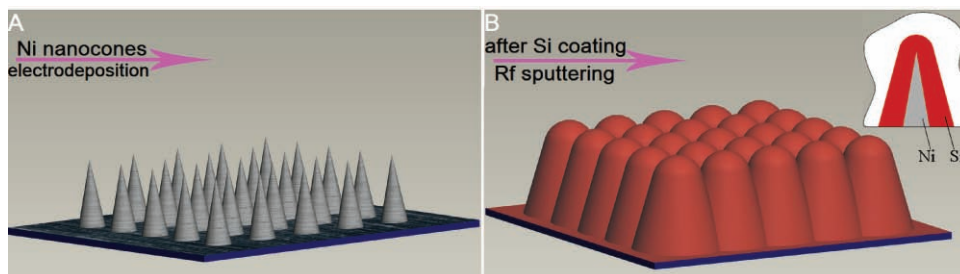


Figure 1. Schematic diagram illustrating the fabrication of a nickel nanocone-array supported silicon anode architecture: A) Nickel nanocone-arrays before Si coating, B) after Si coating.

and Ni cone is well-knit and seamless because the deposition process renders a good adhesion between the deposited coating and the substrate so that they maintain contact during volume changes thereby increasing the cyclability as summarized before.^[6] Energy dispersive X-ray spectroscopy (EDX) was carried out to verify that the amorphous coating was Si, and not SiO_2 , which was confirmed by the absolutely dominant Si and Ni signals with insignificant amounts of impurity (Supporting Information, Figure S3).

After the deposition of the amorphous Si, the Ni NCAs could function directly as current collectors and the amorphous silicon coating acted as the active material so that no other binding or conductive additives were needed. The samples were directly assembled into half-cells with Li metal as the counter electrode to investigate their Li-storage properties. A

cyclic voltammogram of nanostructured Si electrodes is shown in **Figure 3A**. During the first discharge (Li alloying), there was a cathodic peak at around 0.49 V, which disappeared in the subsequent cycles. This cathodic peak can be assigned to the formation of a solid electrolyte interphase (SEI) layer because of decomposition of electrolyte on the Si surface.^[23,24] The charge current associated with the formation of a Li–Si alloy began at a potential of around 0.30 V and became quite large below 0.13 V. Upon discharge, two current peaks appeared at around 0.37 and 0.52 V, which can be ascribed to the phase transition between amorphous Li_xSi and amorphous silicon. These current-potential characteristics are consistent with previous reports on amorphous Si thin-film anodes.^[24]

Figure 3B shows the voltage profiles of nanostructured Si electrodes cycled over a voltage range of 0.01–1.8 V at a current

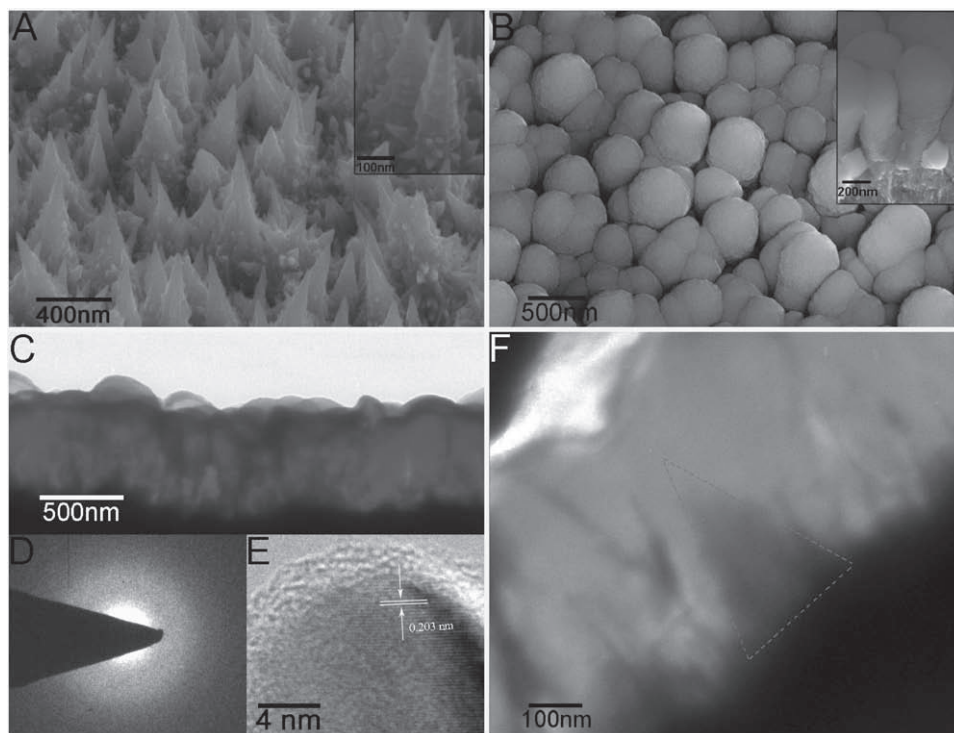


Figure 2. A) SEM image of electrodeposited Ni NCAs. B) Top and cross-sectional (inset) SEM images of Ni NCAs supported Si electrode. C) TEM image of Ni NCAs supported Si electrode. D) SAED image of rf-sputtered Si coating. E) High-resolution TEM image of the Ni cone and Si coating. F) High-magnification TEM image of a single Ni nanocone wedged into the Si coating.

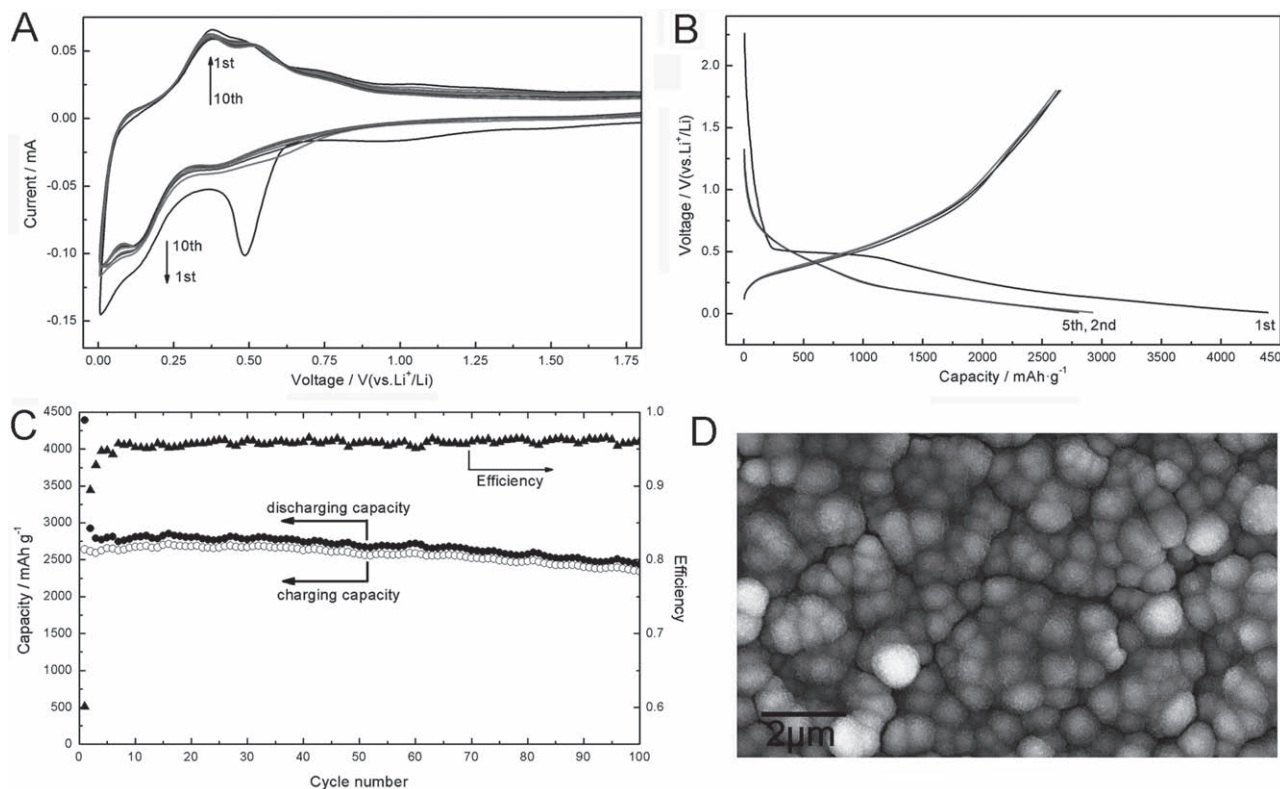


Figure 3. A) Cyclic voltammogram of a nanostructured Si electrode at a scan rate of 0.1 mV s^{-1} (voltage range: 5 mV – 2.5 V) for the first 10 cycles. B) Voltage profiles of the electrode in half cells cycled between 10 mV and 1.8 V versus Li^+/Li at a rate of 0.2 C ($= 0.84 \text{ A g}^{-1}$). C) Discharge (solid circle) and charge (open circle) capacity and Coulombic efficiency (up triangle) versus cycle number for the half cells in Figure 3B. D) SEM images of a nanostructured Si electrode after 50 cycles.

density of 0.84 A g^{-1} (rate = 0.2 C). The first discharge has a short plateau at around 0.50 V up to 1100 mAh g^{-1} , which is the SEI formation potential on a Si surface.^[23,24] The following sloping region gradually dropping to 0.01 V is related to Si lithiation to amorphous Li_xSi (between 1100 and the end of 4391 mAh g^{-1}) with Si lithiation capacity of 3291 mAh g^{-1} . Because the first Si lithiation process (3291 mAh g^{-1}) does not reach the capacity needed for the formation of crystalline $\text{Li}_{15}\text{Si}_4$ (3579 mAh g^{-1}), the first charge shows no plateau originating from delithiation of crystalline $\text{Li}_{15}\text{Si}_4$,^[25,26] as was also the case in Cui's research.^[27] As a matter of fact, the absence of $\text{Li}_{15}\text{Si}_4$ avoids the formation of two-phase regions usually associated with high internal stresses,^[6] thereby resulting in excellent cyclability which will be discussed later. After the first cycle, the discharge and charge profiles show typical behavior (sloping curves) of Li intercalation/extraction into/from the amorphous Li_xSi .^[18,23]

Figure 3C depicts the charge/discharge (rate = 0.2 C) capacity and Coulombic efficiency versus cycle number plots, providing a direct evidence of the excellent lithium storage performance. The first discharge and charge capacity are 4391 and 2640 mAh g^{-1} (approximately 7 times that of commercial graphite), with a low initial Coulombic efficiency of 60.1% . The irreversible capacity ratio of 39.9% can be assigned to the initial formation of a SEI layer on the electrode surface as discussed above, and to the irreversible insertion of Li

ions into the silicon coating. However, the efficiency gradually increases in the following cycles (ca. 95% for cycles 4 – 20 , ca. 96% for cycles 20 – 100). This can be ascribed to the fact that the Ni NCAs are deeply wedged into the Si coating, which maintains a direct electrical connection with the substrate, thereby shortening the diffusion distance for lithium insertion and facilitating electron collection and transport. The reversible capacity gradually increases from the second cycle onward and reaches its highest value of 2714 mAh g^{-1} in the 16th cycle because in each cycle additional material is activated to react with Li.^[28] Subsequently, the reversible capacity reduces very slowly. For example, the charge capacity for the 20th cycle was 2683 mAh g^{-1} and that for the 100th cycle was 2341 mAh g^{-1} , leaving a retention rate of 87.3% , or 99.8% per cycle. This improved electrochemical performance is attributed to the optimized Si/Ni configurations in which the inactive Ni matrix as well as the space between each cylinder acts as the confining buffer to accommodate the enormous volume changes and alleviate the concomitant huge stresses owing to repeated Li alloying/dealloying with Si. Furthermore, the fact that the Ni NCAs are wedged into the Si coating strengthens the bonding force between the current collector and the active materials. The excellent cyclability is comparable to that of recent research on a nanostructured silicon composites anode,^[17–20] however, our anodes are more simple and economical to make.

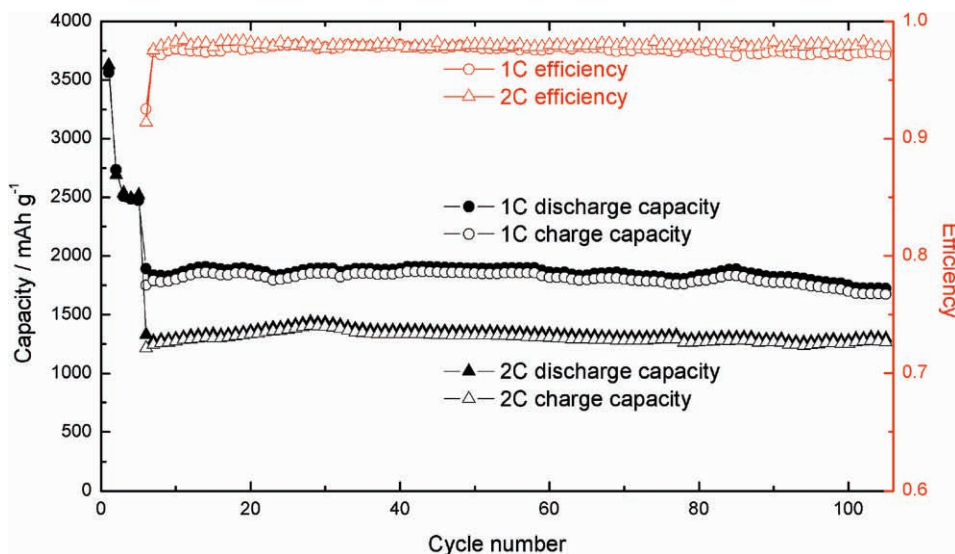


Figure 4. Discharge/charge capacity and Coulombic efficiency versus cycle number for a nanostructured Si electrode at 1 C and 2 C rates after 0.2 C for 5 cycles with a cut-off voltage of 10 mV–1.6 V.

To determine whether the morphology of the nanostructured Si electrode had changed after repeated lithium alloying/dealloying, one cell was disassembled after 50 cycles (charging up to 1.8 V) for SEM characterization of the electrode as shown in Figure 3D. Compared to the image of the pristine sample, the morphology shows less variation. The gaps between each cylinder became indistinct whereas some crevices can be seen to form small coordinated regions randomly on the surface with sizes of about 1–4 μm . With a volume expansion of over 300% because of Li–Si alloying, the Si/Ni cylinders agglomerate; after Li–Si de-alloying, they shrink again, however not to the original morphology but preferably into self-adjusted flakes to relieve the stresses inside the Si coating. Eventually, the film does not disintegrate and degrade because the Ni NCAs stick to the Si coating tightly and therefore the coating is not shed off. This proves the advantage of our well-designed nanostructured Si electrodes over pure Si films with thicknesses of 250 nm, in which excellent capacity retention for only 30 cycles was followed by rapid fading and electrode collapse.^[16]

Owing to the well-aligned Ni NCAs, which work as good mechanical supports and efficient electron pathways, the nanostructured Si electrode is expected to make high rate capability feasible. Figure 4 illustrates the cycling performance of the anodes up to the 105th cycle at 1 C (4.2 A g^{-1}) and 2 C (8.4 A g^{-1}) rates. A slow rate of 0.2 C was operated at the beginning for five cycles to condition and expand the electrodes slowly as reported before.^[17,20] There is a capacity drop of about 23% when the cycling rate was increased from 0.2 C to 1 C. The charge capacity at 1 C started at 1750 mAh g^{-1} and still attained 1674 mAh g^{-1} after 105 cycles with a retention of 95.6%. The cell exhibited a good Coulombic efficiency of 93% for the 6th cycle and a high efficiency of >97% afterwards. Similarly, the cycling capability at 2 C was also excellent with a charge capacity of 1215 mAh g^{-1} for the 6th cycle. The capacity increased progressively to 1404 mAh g^{-1} for the 28th cycle and retained 1267 mAh g^{-1} after 105 cycles with a slight decrease of about 0.13% per cycle.

High Coulombic efficiencies for the 7th–105th cycle (97.5–98.5%) were observed as well. Additionally, it only took 9 min to charge/discharge the nanostructured Si anode at the 2 C rate (Supporting Information, Figure S4), corresponding to a factual rate of 6.5 C. This increased rate is related to the significantly lower capacity compared to the theoretical capacity of Si.

In summary, we have successfully synthesized a Ni NCAs supported Si architecture composed of many cylinders with regular domes on top to serve as the anode material for Li-ion batteries. In this configuration, the Ni NCAs facilitate charge collection and transport, support the electrode structure, and function as inactive confining buffers. These nanostructured Si electrodes show impressive electrochemical performance, with a high capacity of around 2400 mAh g^{-1} (at 0.2 C rate) over 100 cycles with superior capacity retention of 99.8% per cycle. They also exhibit excellent lithium storage capability at high charging and discharging rates. We believe that this configuration design may be exploited for other active materials to achieve a high-capacity, high-rate, and durable electrode for Li-ion batteries.

Supporting Information

Supporting Information is available from the Wiley Online Library or from the author.

Acknowledgements

This work was supported by the National Natural Science Foundation of China (50954005, 51074011), the National Basic Research Program of China (2007CB936502), and the National 863 Program (2006AA03Z230, 2008AA03Z208).

Received: August 19, 2010
Published online: October 14, 2010

- [1] J.-M. Tarascon, M. Armand, *Nature* **2001**, 414, 359.
- [2] A. S. Arico, P. Bruce, B. Scrosati, J.-M. Tarascon, W. Van Schalkwijk, *Nat. Mater.* **2005**, 4, 366.
- [3] M. Armand, J.-M. Tarascon, *Nature* **2008**, 451, 652.
- [4] B. A. Boukamp, G. C. Lesh, R. A. Huggins, *J. Electrochem. Soc.* **1981**, 128, 725.
- [5] P. Poizot, S. Laruelle, S. Grugeon, L. Dupont, J.-M. Tarascon, *J. Power Sources* **2001**, 97–98, 235.
- [6] U. Kasavajjula, C. S. Wang, A. J. Appleby, *J. Power Sources* **2007**, 163, 1003.
- [7] R. A. Huggins, *J. Power Sources* **1999**, 81–82, 13.
- [8] A. Netz, R. A. Huggins, W. Weppner, *J. Power Sources* **2003**, 119–121, 95.
- [9] G. X. Wang, L. Sun, D. H. Bradhurst, S. Zhong, S. X. Dou, H. K. Liu, *J. Power Sources* **2000**, 88, 278.
- [10] B. C. Kim, H. Uono, T. Satou, T. Fuse, T. Ishihara, M. Ue, M. Senna, *J. Electrochem. Soc.* **2005**, 152, A523.
- [11] Y. Zhang, X. G. Zhang, H. L. Zhang, Z. G. Zhao, F. Li, C. Liu, H. M. Cheng, *Electrochim. Acta* **2006**, 51, 4994.
- [12] N. Dimov, S. Kugino, A. Yoshio, *J. Power Sources* **2004**, 136, 108.
- [13] H. Y. Lee, S. M. Lee, *Electrochem. Commun.* **2004**, 6, 465.
- [14] H. Li, X. Huang, L. Chen, G. Zhou, Z. Zhang, D. Yu, Y. J. Mo, N. Pei, *Solid State Ionics* **2000**, 135, 181.
- [15] J. Graetz, C. C. Ahn, R. Yazami, B. Fultz, *Electrochem. Solid-State Lett.* **2003**, 6, A194.
- [16] J. P. Maranchi, A. F. Hepp, A. G. Evans, N. T. Nuhfer, P. N. Kumta, *J. Electrochem. Soc.* **2006**, 153, A1246.
- [17] L. F. Cui, Y. Yang, C. M. Hsu, Y. Cui, *Nano Lett.* **2009**, 9, 3370.
- [18] L. F. Cui, R. Ruffo, C. K. Chan, H. L. Peng, Y. Cui, *Nano Lett.* **2009**, 9, 491.
- [19] W. Wang, P. N. Kumta, *ACS Nano* **2010**, 4, 2233.
- [20] S. Zhou, X. Liu, D. Wang, *Nano Lett.* **2010**, 10, 860.
- [21] T. Hang, M. Li, Q. Fei, D. Mao, *Nanotechnology* **2008**, 19, 035201.
- [22] T. Hang, A. Hu, H. Ling, M. Li, D. Mao, *Appl. Surf. Sci.* **2009**, 256, 2400.
- [23] H. Xia, S. Tang, L. Lu, *Mater. Res. Bull.* **2007**, 42, 1301.
- [24] L. B. Chen, J. Y. Xie, H. C. Yu, T. H. Wang, *J. Appl. Electrochem.* **2009**, 39, 1157.
- [25] T. D. Hatchard, J. R. Dahn, *J. Electrochem. Soc.* **2004**, 151, A838.
- [26] M. N. Obrovac, L. Christensen, *Electrochem. Solid-State Lett.* **2004**, 7, A93.
- [27] L. F. Cui, L. Hu, J. W. Choi, Y. Cui, *ACS Nano* **2010**, 4, 3671.
- [28] M. Green, E. Fielder, B. Scrosati, M. Wachtler, J. S. Moreno, *Electrochem. Solid-State Lett.* **2003**, 6, A75.